

J. Kej. Awam Jil. 8 Bil. 2 1995

**MODELLING OF SHEAR IN POST-TENSIONED
BRICKWORK CANTILEVER FIN WALLS**

by

Dr. Faridah Shafii

Department of Structures & Material
Faculty of Civil Engineering

Abstract

This paper describes a model scale investigation of the shear behaviour of post-tensioned brickwork cantilever fin walls. The developments of models to represent the critical region under shear are described. Details of reduced height test walls to simulate the actual forces and critical shear zone are presented. It is concluded that the shear behaviour of prestressed walls can be studied by modelling at reduced scale.

1.1 Introduction

In post-tensioned walls the resistance to horizontal loads is provided by both the bending and shear strength of the wall. However, although the presence of prestress force improves the shear strength, it is often shear rather than bending which governs the load-carrying capacity, especially for earth retaining walls with geometric cross-sections. For a wall subjected to lateral load, the combined effects of bending moment, shear force and axial load can produce principal stresses which are more critical than those created by the individual forces. In geometrical sections, where the webs are relatively thin, these may lead to the development of diagonal cracking of the web. So far, only a small amount of research has been done to explore this particular problem in post-tensioned brickwork [Roumani and Phipps (1988), Curtin, Shaw and Howard (1991), Hobbs and Shafii (1992), Shafii (1994)]. The work reported in this paper was part of an investigation undertaken to study the shear behaviour of post-tensioned cantilever fin walls.

The majority of existing experimental research on post-tensioned walls has been based on testing full scale brickwork. This requires considerable time and effort in the preparation and construction of test specimens and consequently restricts the number of tests that can be undertaken during the period of research. Additionally, full scale testing may also be restricted by the availability of laboratory facilities and space to accommodate the brickwork structure. Previous research by Hobbs and Daou (1988, 1993) investigated the behaviour of free cantilever fin walls subjected to lateral loading using model scale studies. It was concluded that with a proper modelling system, model testing could offer an alternative to full scale test therefore allowing wider range of tests to be undertaken at much reduced cost and time. The advantages gained from model testing include the ability to test up to the ultimate stage of failure, while full scale tests may be restricted to lower levels of applied load due to the risk of a dangerous collapse. The work conducted by Hobbs and Daou (1988, 1993) identified shear as the critical mode of failure requiring further investigation.

The development of models to represent the critical region under shear is discussed in this paper. Details of reduced height test walls to simulate the actual forces and stresses in the critical shear zone are presented together with the methods of testing. The structural performance and cracking behaviour of these test specimens are examined in relation to a full height wall.

2.0 Material properties

2.1 Bricks

The model bricks used were manufactured in accordance to the specifications of high quality solid, clay engineering bricks and cut to correspond to a scale of 0.293 based on the nominal dimensions of a British Standard brick. The mean dimensions based on a representative sample of ten bricks selected at random from the batch were 64.21 x 29.93 x 18.52 mm for the length, width and height respectively. The mean value of the initial rate of suction (IRS) and water absorption of ten bricks determined in accordance to BS 3921 was 0.378 kg/m²/min and 3.71% respectively. The mean compressive strength of the bricks when tested on bed, stretcher and header directions were 127 N/mm², 95 N/mm² and 87 N/mm² respectively. The mean tensile strength of the bricks when tested in direct tension applied to the header faces was 8.4 N/mm².

2.2 Mortar

The mix was designed to conform to mortar designation (i) as specified in BS 5628 ; part 1 : 1978 using ordinary portland cement. Sand particles smaller than 1.18 mm were used so that the sand were not disproportionately large to the 3 mm mortar joint of the model brickwork. The mix proportions by weight were cement, 1 : lime, 0.134: and sand 3.887 with a water to cement ratio of 0.97. The mean compressive strength of the mortar at 28 days was 17.82 N/mm² with an elastic modulus of 14.9 kN/mm².

2.3 Prestressing steel

High tensile grade EN26 steel bars with nominal diameter of 22 mm and cross-sectional area of 380 mm² were used as the prestressing tendon. The mean elastic modulus of the steel determined from the results of 3 specimens was 213 kN/mm² whilst the mean ultimate tensile strength was 1032 N/mm².

3.0 Development of wall section and construction

A section geometry similar to that used by Hobbs and Daou (1988, 1993) was adopted in order that comparison of results could be made between the models established in this investigation and the previous work. The T-shaped section is shown in Fig.1. Calculations of the elastic section properties were based on the cross section of the brickwork taking into account of the presence of the void in the web. The calculated resultant stresses on the outer fibre of the flange face, f_1 and the web face, f_2 , at the end of the prestressing operation were 0.3 N/mm² and 10.60 N/mm² respectively. Based on the recommendations of the code, BS 5628 : part 2 : 1985, the value of f_k was determined from compression testing of stretcher bond wallettes. This gave a mean strength of 47 N/mm². Specimens were also sawn from the flange sections of the walls after testing and these gave a mean compressive strength of 52 N/mm².

The bonding arrangements for the wall section is shown in Fig. 2. The bonding pattern was designed to minimise the number of internal straight joints. Wall specimens were constructed on a reinforced concrete base which was secured to the loading rig. A steel jig was used to guide the brickwork construction in order to maintain the joints and alignment at the required position. The specimens were cured for 28 days prior to testing.

4.0 Establishment of model and loading arrangements

The present research deals with the shear behaviour, therefore it was necessary to concentrate studies on the critical portion of the wall. The tests were based on a notional full scale wall of 5.0 m height, giving a scaled height of 1.5 m.

Investigations were undertaken to study the general behaviour of short walls, representing the lower part of the full height in relation to a full height scale model wall. The first stage of testing was to establish a model and loading system which would generate similar shear behaviour to a full height wall. This series of test determined the height of specimen and appropriate loading arrangements necessary to reproduce the stresses expected in a full scale wall. The second stage of testing was to confirm the applicability of the above test method in simulating the behaviour of other test walls, similar to the ones reported by Hobbs and Daou (1988, 1993).

General details of the wall construction and prestressing arrangement are given in Fig. 3. The loading arrangements, and the corresponding shear force and bending moment diagrams of the models are shown in Fig. 4 to Fig. 6. Walls B3, B5 and B6 in Fig. 4 were used as references. The three reference walls were identical except for the initial prestress force used. The geometrical and loading arrangements shown in Figs. 5 and 6 were investigated to establish a suitable method of reproducing the shear behaviour of a full height wall. Full details of the instrumentation and the testing procedures have been given by Shafii (1994).

5.0 Test results and discussions

5.1 Mode of failure

The walls tested in this investigation failed by shear cracking of the web preceded by flexural cracking which started at the base of the wall when the flexural tensile strength of the brickwork was reached. As the lateral load increased the crack propagated through the web towards the compression flange.

The first diagonal crack occurred at some point in the web, independently and away from the flexural crack, when the critical value of the principal tensile stress was reached. As the load increased, the diagonal crack propagated through bricks and along mortar joints and extended diagonally towards the load point and then downwards to the compression zone. The subsequent propagation of cracks resulted in extensive damage to the web.

5.2 Load-deflection response

A typical graph of the load deflection behaviour of the test walls is shown in Fig. 7. In general, during loading the walls exhibited three principal stages of behaviour. The first stage O-X represents the stage of the wall behaviour before flexural cracking. At this elastic stage the deformations of the wall are more or less linearly proportional to the applied moment, i.e linear elastic behaviour. The slope of the linear portion is a measure of the uncracked elastic stiffness of the wall. The end of this stage was marked by flexural cracking.

Afterwards, a short transition stage (X-Y) occurs in which the wall stiffness reduced rapidly as the flexural crack at the base of the wall penetrated towards the compression face. The crack propagated rapidly with only a small increase in the lateral load, thus causing a marked change in gradient of the curve.

The second stage (Y-Z) is characterised by an increased rate of deflection with applied load and represents the behaviour of the wall after the flexural crack occurs and while the steel stress is still in the elastic range. There is a proportional increase in deflection with load beyond point Y, an indication that although the walls cracked, they continued to behave elastically. With increase in applied load, the flexural crack at the bottom of the wall progressed towards the flange and the wall rotate at the bottom of the wall around the compression zone.

Point Z marks the end of the second stage where the curve diverted from linearity due to the appearance of shear failure in the form of diagonal cracking.

The third stage of the load-deflection curve is characterised by a very slow change in slope. Point V in Fig. 7, corresponds to the maximum applied load on the wall. In most cases, tests were carried through to failure until reaching point V. However, for wall T1A150, where the prestress force in the tendon approached the elastic linear limit of steel, test was undertaken to reach as far as possible beyond point Z.

5.3 Brickwork stresses at failure

The applied load in the walls at the critical stages of testing and the brickwork stresses at shear failure are shown in Table 1 and Table 2 respectively. The crack patterns in typical walls are shown in Fig. 8.

The flexural cracking load of walls R1A150, U1A150 and S1A150 appear to be of similar order to wall B6 with the exception of wall T1A150, Table 1. Flexural cracking occurred when the stresses on the extreme fibre of web exceed the flexural tensile strength of the brickwork. Theoretically the flexural tensile strength should be a constant for brickwork made of the same materials, but variations could occur with qualities and variability of materials. The calculated flexural tensile strength based on elastic analysis for wall R1A150, U1A150 and S1A150 varied up to 0.8 N/mm^2 . The result of wall T1A150 is inconsistent from the other walls and this could be due to the very small shear span or possibly an experimental error causing delay in detecting the crack at the instant when the first crack appear.

For walls with similar section and subjected to the same prestress force level, the shear behaviour is mainly dependent upon the forces acting on the walls and shear span of brickwork. The forces acting on wall R1A150 were significantly different from wall B6 as illustrated by the bending and shear force diagram in Fig. 5 and Fig. 4 respectively. The shear span of brickwork under maximum shear loading for R1A150 was also larger than wall B6. Previous research [Roumani and Phipps (1988) and Hobbs and Daou (1988, 1989, 1993)] indicated the significance of shear span to the depth ratio on the shear strength of prestressed brickwork. As a_v/D increases the observed shear strength of brickwork decreases. This is evident in Table 2 where the centroidal stresses and principal stresses at first diagonal cracking for R1A150 were smaller than those for B6. At ultimate the strength of B6 was approximately 13% higher than R1A150. The shear crack pattern of wall R1A150 up to the ultimate stage is presented in Fig. 8a.

Wall U1A150 and T1A150 were subjected to lateral load applied on to the capping beam with the resulting shear force and bending moment diagram as shown in Fig. 6. Although the shear span of wall U1A150 was only marginally smaller than R1A150, however, the moment at diagonal cracking was noticeably increased by 11%. In the case of wall T1A150 the shear span was shorter than wall B6. As indicated in Fig. 6b a moment of 0.246 V was induced at the top of brickwork. The first diagonal cracking occurred at a high applied shear force of 84 kN. At the maximum applied shear force, the crack in the web was still at an initial stage of development, Fig. 8c.

Wall S1A150 was constructed to simulate more closely the forces in wall B6. The first diagonal cracking occurred at a shear force corresponding to a moment and a prestress force in the tendon only 4% lower than B6. The shear strength of brickwork at diagonal cracking was also similar to B6, Table 2. The differences in the values of the principal stresses are also negligible considering the effect of material variability and differences in workmanship qualities. The shear crack at failure for walls S1A150 and B6 is given in Fig. 8d and Fig. 8e, and the similarity in the patterns of the main cracks is apparent.

The reliability of the model above was confirmed when it was used in testing walls of identical section for other prestress levels, namely 50 kN and 100 kN, as in walls B3 and B5 tested by Hobbs and Daou (1988, 1989 and 1993). The reduced height model S1A50 and S1A100, produced similar results to B3 and B5 respectively, Table 1 and Table 2. It can also be seen from these tests that increasing the prestress force level tend to increase the flexural cracking and the shear cracking load of the walls. Consequently, the centroidal stresses and principal stresses at first diagonal cracking also increased.

6.0 Conclusions

1. The results of this investigation indicated that shear behaviour is mainly dependent upon the forces acting on the walls and the shear span of the brickwork, a_v , under loading. Decreasing the a_v/D ratio enhanced the shear strength of the prestressed brickwork and this corresponds with the findings of others who have tested full height, full scale walls.
2. As expected increasing the prestress force level increases the flexural cracking load.
3. An increase in prestress force level improved the shear strength at first diagonal cracking and the principal tensile stress at failure.
4. With careful test design it is possible to reproduce the shear behaviour of full height walls by using reduced height specimens representing the lower part of the brickwork only.
5. The shear behaviour of prestressed walls can be studied by modelling at reduced scale, the lower portion of the wall subjected to the critical stresses. This method of testing reduces the specimen size which enables it to be constructed in comparatively shorter time. Additionally, the model walls can be designed to suit the capacity of the available laboratory equipment and testing can be undertaken to reach the ultimate stage with much reduced risk to safety.

Acknowledgements

The authors wish to express their thanks to Messrs Marshalls Clay Products for the supply of the model bricks and technical staff of the University of Sheffield, Department of Civil and Structural Engineering for their willing assistance. The financial support afforded to the first author by The Association of Commonwealth Universities / British Council is gratefully acknowledged. Finally, thanks are also due to Universiti Teknologi Malaysia for granting study leave to carry out the research.

References

- Curtin, W.G., Shaw, G. and Howard, J., Structural testing of a post-tensioned brick fin wall, 9th Int. Brick/Block Masonry Conference, Berlin, 1991, Vol. 1, pp 333-343.
- Daou, Y.A., Behaviour of post-tensioned brickwork cantilever fin walls, PhD Thesis, University of Sheffield, 1989.
- Hobbs, B. and Daou, Y.A., Post tensioned T-section brickwork retaining walls, Proc. 8th Int. Brick and Block Masonry Conference, Dublin, Sept. 1988, pp 665-675.
- Hobbs, B. and Daou, Y.A., An experimental investigation of post-tensioned brickwork fin walls, Proc. Inst. of Civil Engineers, Building and Structures, 1993.
- Hobbs, B. and Shafii, F., Application of post-tensioning to brickwork retaining walls, Asia-Pacific Structural Engineering Conference, Universiti Teknologi Malaysia, Sept., 1992.
- Roumani, N. and Phipps, M.E., The ultimate shear strength of unbonded prestressed I and T section simply supported beams, Proc. Br. Ceram. Soc. Masonry (2) Stoke-on-Trent, No. 2, April 1988, pp 82-84.
- Shafii, F., Shear behaviour of post-tensioned brickwork cantilever fin walls, PhD Thesis, University of Sheffield, 1994.

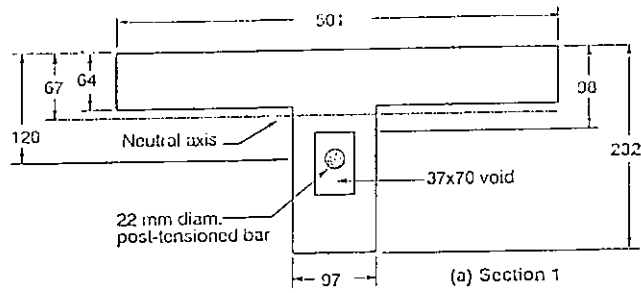


Fig. 1 Section of wall

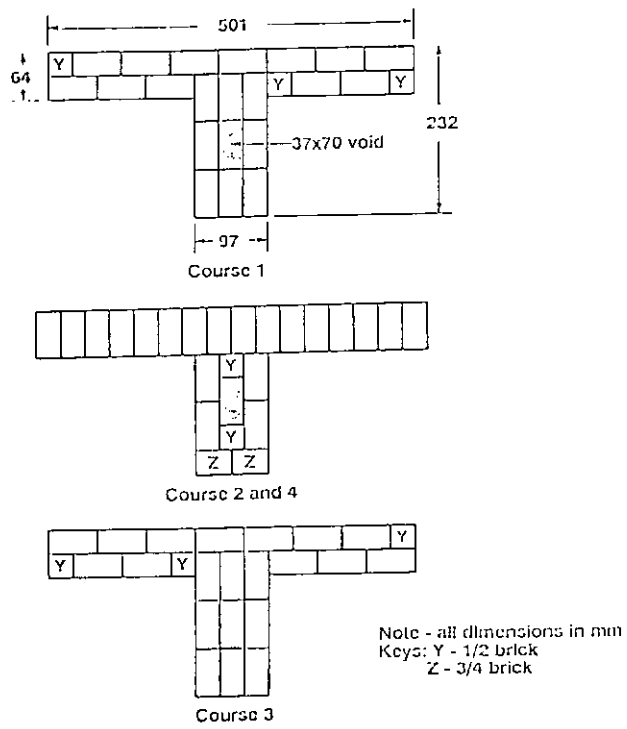


Fig. 2 Bonding arrangement

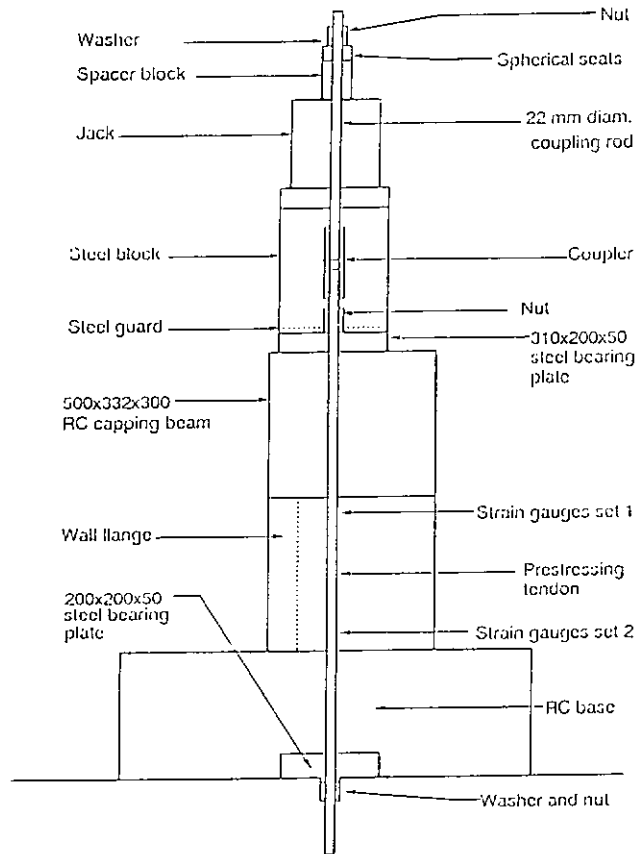


Fig. 3 Section through test assembly

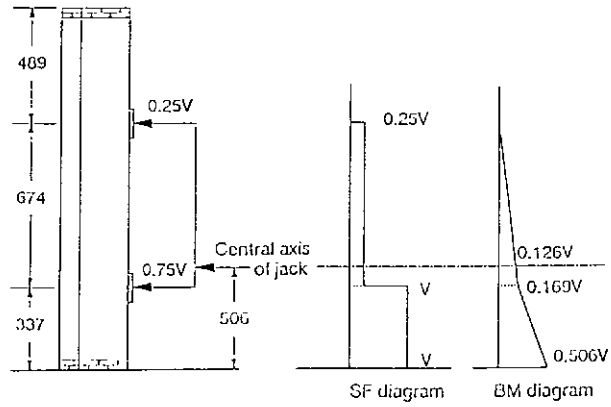


Fig. 4 Shear force and bending moment diagram of reference walls (B3, B5 and B6)

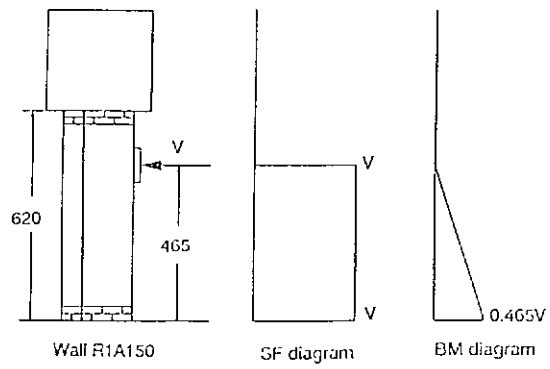
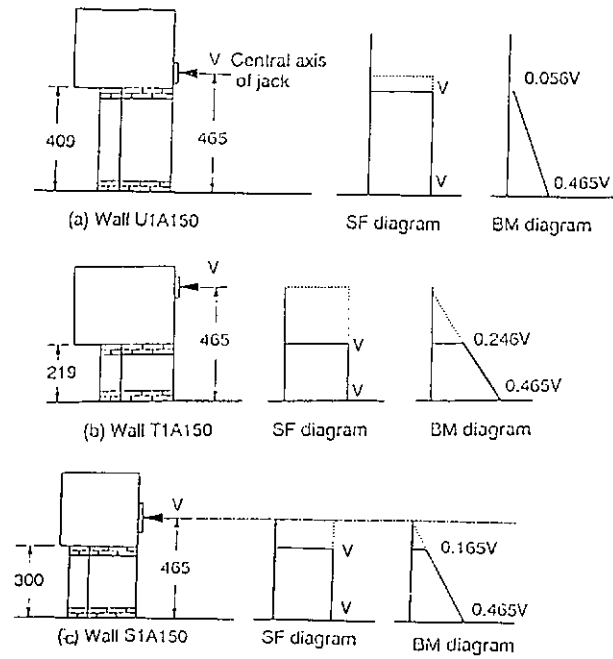


Fig. 5 Shear force and bending moment diagram of wall R1A150



Note: All dimensions in mm

Fig. 6 Shear force and bending moment diagram of wali U1A150, T1A150 and S1A150

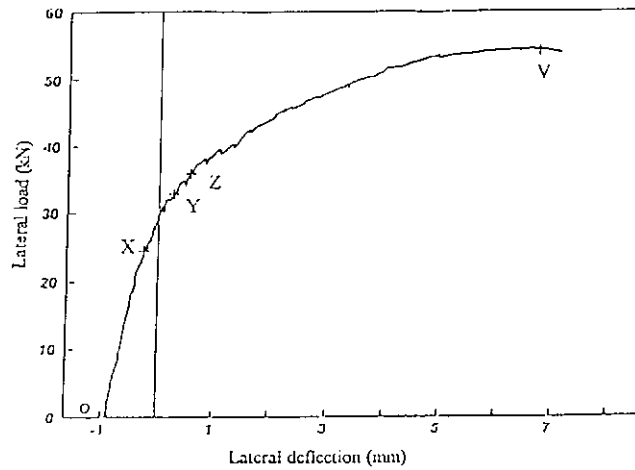
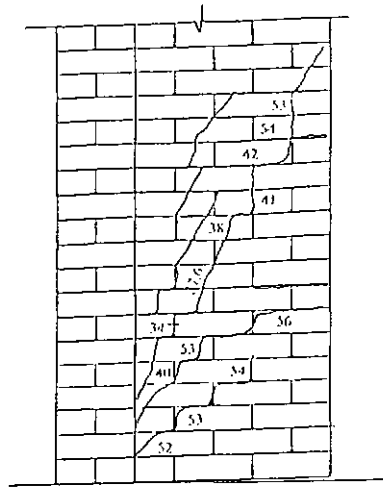
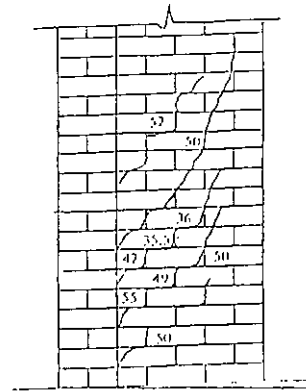


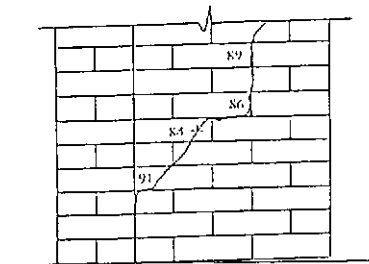
Fig. 7 A typical load-deflection curve of test wall



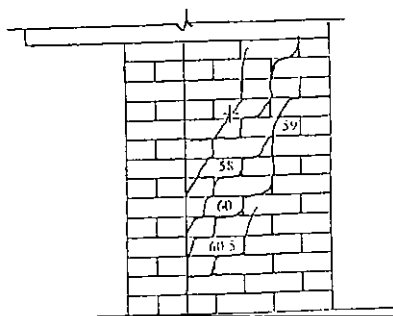
(a) RIA150



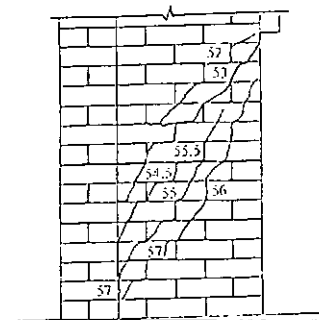
(b) UIA150



(c) TIA150



(d) SIA150



(e) B6

Fig. 8 Shear crack pattern of test walls

| Walls | Initial prestress force (kN) | N/V | a, (mm) | a/D | Flexural cracking | | | Diagonal cracking | | | Ultimate | | | Failure mode |
|--------------------------------------|------------------------------|-------|---------|------|-------------------|----------------|-----------------|-------------------|------------------|------------------|----------------|----------------|----------------|---|
| | | | | | P _s | V _c | M _{cr} | P _{1/2} | V _{1/2} | M _{1/2} | P _u | V _u | M _u | |
| | | | | | | | | | | | | | | |
| Dadu (1989) B6 B5 B3 | 150 | 0.506 | 312 | 1.35 | 153.60 | 28.33 | 14.33 | 216.00 | 54.15 | 27.41 | 219.90 | 59.37 | 30.04 | Flexural tensile crack occurred at the base of wall, and followed by diagonal cracking of the web |
| | 100 | | 312 | 1.35 | 105.00 | 16.48 | 8.34 | 203.00 | 50.00 | 25.30 | 212.00 | 53.33 | 26.98 | |
| | 50 | | 312 | 1.35 | 52.20 | 7.37 | 3.73 | 163.00 | 41.66 | 21.08 | 136.07 | 48.33 | 24.45 | |
| RIA150 UA150 *TIA150 SIA150 | 150 | | 415 | 1.79 | 154.47 | 28.00 | 13.02 | 155.00 | 32.00 | 14.88 | 212.32 | 56.37 | 26.21 | Flexural tensile crack occurred at the base of wall, and followed by diagonal cracking of the web |
| | 150 | 0.465 | 409 | 1.76 | 131.85 | 26.00 | 12.07 | 154.00 | 35.50 | 16.51 | 210.00 | 60.00 | 27.90 | |
| | 150 | | 219 | 0.94 | 200.00 | 43.00 | 20.00 | 271.70 | 84.00 | 39.06 | *207.00 | *95.00 | *14.18 | |
| SIA100 SIA50 | 150 | | 300 | 1.29 | 152.86 | 26.00 | 12.09 | 209.54 | 57.50 | 26.73 | 211.70 | 63.30 | 29.43 | |
| | 100 | 0.465 | 300 | 1.29 | 106.64 | 18.00 | 8.37 | 197.54 | 53.00 | 21.65 | 210.26 | 56.31 | 26.18 | |
| | 50 | | 300 | 1.29 | 53.10 | 9.50 | 4.12 | 152.26 | 38.00 | 17.67 | 116.57 | 54.60 | 25.39 | |

Notes: P - prestress force in tendon (kN)
V - Shear force (kN)
M - moment (kNm)
* Wall not tested to ultimate failure

Subscripts: α - flexural cracking
β - diagonal cracking
γ - ultimate

Table 1. Test results at the critical stages of loading

| Walls | a, /D | Centroidal stresses, N/mm ² | | Principal stresses, N/mm ² | |
|--------|-------|--|-----------------|---------------------------------------|---------------------|
| | | Compression f_c | Shear τ | Compression f_{pc} | Tension f_{pt} |
| B6 | 1.35 | 4.46 | 3.39 | 6.45 | 2.00 |
| D5 | 1.35 | 4.19 | 3.35 | 6.05 | 1.86 |
| H3 | 1.35 | 2.79 | 2.79 | 4.94 | 1.58 |
| R1A150 | 1.79 | 3.43 | 2.08 | 4.41 | 0.98 |
| U1A150 | 1.76 | 3.55 | 2.30 | 4.68 | 1.13 |
| T1A150 | 0.94 | 5.99 | 5.45 | 9.21 | 3.22 |
| S1A150 | 1.29 | 4.62 | 3.73 | 6.70 | 2.08 |
| S1A100 | 1.29 | 4.36 | 3.44 | 6.25 | 1.89 |
| S1A50 | 1.29 | 3.37 | 2.47 | 4.68 | 1.30 |

Notes: The compressive stress at the centroid was calculated taking into account of the weight of capping beam

Table 2 Stresses at shear failure